Engineering Journal issn: 0125-8281

Article

Design and Investigation of Miniature Solar Cell Source Inductive Wireless Power Transfer on Various Distances, Turns and Loads

Waluyo[a,*], Syahrial[b], and Fathurrahman Yasin[c]

Department of Electrical Engineering, Institut Teknologi Nasional Bandung (Itenas), Jalan PHH. Mustafa No. 23 Bandung 40124 West Java, Indonesia
E-mail: [a]waluyo@itenas.ac.id (Corresponding author), [b]syahrial.electrical@gmail.com, [c]fathur.phoenix@gmail.com

Abstract. The research was to transfer the electric power from a photovoltaic module in wireless utilized magnetic coupling method and an inverter. It was also investigated the waveform characteristics due to various distances, turns and loads. The measurements were performed by using a storage digital oscilloscope, to obtain the voltage magnitudes and harmonics. The results indicated that the receiver voltage magnitudes would decrease drastically, in hyperbolic curves, as the distance increased. The receiver voltage magnitudes would also decrease considerably as the turns reduced, with the average reductions as 0.095 and 0.357 volts, from 600 to 400 and 400 to 200 turn reductions respectively. The THDs in the transmitter voltages were fairly constant, as average of 26.75%. Nevertheless, the receiver voltage THDs would decrease significantly as the distance increased, with decreasing average as 38.09% of the three condition percentage reductions. While, the THDs would reduce considerably as the turns decreased, as 25.28% in average for the 200 to 400, and 400 to 600 turns on one cm of distance. Otherwise, the voltage magnitudes would decrease as the loads increased where from one to five lamp loads, as 0.489, 1.334 and 1.482 volts reductions for 200, 400 and 600 turns respectively. The THDs would decrease slightly as the loads increased, with the average reduction of 5.4% from one to five lamp loads, for the three turn conditions. The receiver voltage magnitudes would increase steep linearly, with the average ratio of one per 9.30 as the transmitter voltage magnitudes increased. While, the THDs of receiver voltages would reduce considerably as the transmitter voltage magnitudes increased, with 8.98% reduction for 1.4 to 5.2 volts of the transmitter voltage magnitudes.

The receiver power would reduce more drastically, compared to the voltages, as the distance increased. This case was caused which the powers were influenced by both electric voltage and current. The efficiency would also reduce drastically as the distance increased. Nevertheless, it was gentler than the power, because the early values have already been low. Both parameters were significantly influenced by the coil turns, which the efficiency would be lower as the coil turns reduced. Based on the research results, the maximum transferring efficiency was 0.0615. The efficiency would slightly increase and tended to be saturated toward a certain value as the load increased. Therefore, most likely, in the future, the coil turns should be increased.

Keywords: Efficiency, harmonics, magnetic coupling, power, receiver, photovoltaic, THD, transmitter, turn, voltage, wireless.

ENGINEERING JOURNAL Volume 22 Issue 4
Received 7 November 2017
Accepted 4 May 2018
Published 31 July 2018
Online at http://www.engj.org/
DOI:10.4186/ej.2018.22.4.121

DOI:10.4186/ej.2018.22.4.121

1. Introduction

Conservation and environmental friendly energy products become strong underlying issues of global energy development policy. Solar energy is one of renewable energy and environmentally clean. The solar energy is also used as heat energy. Indonesia is a tropical country, has great potential for solar energy, an average of 4.5 to 4.8 kWh/m^2/day. It was stated that the solar energy in Indonesia as 156,487 MW. This is very potential to be used in electric demand in the view of problem severity with fossil-based power generation. On the other hand, over the times, human need on energy is inevitable, because energy is a primary need [1-9]. Photovoltaic panels have many applications, one was for office appliances and it needs to be diagnosed [10-11].

The researches on wireless electric power transmission were to be encouraged, because of economic considerations compared to cables. Some methods of transmission system power were inductive coupling, inductive coupling resonance, capacitive coupling, magneto dynamic coupling and radioactive techniques [12-20].

The applications of wireless power transfer are for low-power, full power, high power and in industry. Electric current can be postulated as a stream of electromagnetic waves having electric potential. The wireless energy transmission at a low level is not harmful to the human body. The advantages of wireless power transmission, among others, can be transmitted in all directions, low installation cost, more reliable and convenient, environmentally friendly, minimize accidents, relatively safe. The disadvantage is the efficiency decreases as distance between transmitter and receiver increases. The inductive and inductive resonance wireless power transfers have significant attention [14, 21-28].

The electric energy of wireless transmission can cover widely in electrical engineering and electronics to the scope in the future for the generation and power transfer in wireless [29-40]. Wireless power transfer also could be done with a helical antenna. This method needs to be done further research and testing [41]. Even the wireless electric power transfer can also use satellite-based solar power system [42].

The magnetic or inductive coupling works on the principle of electromagnetism. Transfer of energy is among wires through the magnetic field inductive coupling. If a section is defined by the magnetic flux circuit that covered by the second set, the two circuits are coupled magnetically. The energy can be transferred from one to other circuits. This energy transfer is conducted by the transfer magnetic field which applies to both circuits [43].

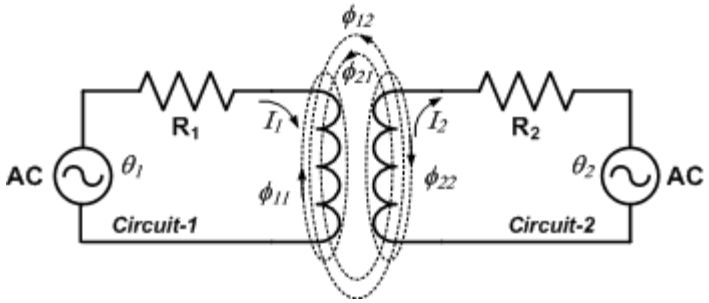

Fig. 1. Magnetic coupling with four flux components.

The magnetic coupling between the two circuits is shown in Fig. 1. For analysis purposes, it is assumed that the total flux set by i_1 (current circuit 1) is divided into two components. The part one links to the circuit 1, but not with the circuit 2. The second component is surrounded by both circuit 2 and circuit 1. In the same way, the flux is determined by i_2 (current of circuit 2), that has two components. One component 2 is 22 which linkages only the circuit 2 but not to circuit 1. The other component than 2 is 21 which linkages both the circuit 2 and the circuit 1. Equations (1) and (2) show the relations among flux linkages.

$$\phi_1 = \phi_{11} + \phi_{12} \tag{1}$$

$$\phi_2 = \phi_{22} + \phi_{21} \tag{2}$$

Here, ϕ_{12} is part of ϕ_1, which linkages the coil circuit 2. Therefore, ϕ_{12} is called a mutual flux generated by the circuit 1. In the same way, the fractional part of ϕ_2 is ϕ_{21} that connecting with the coil circuit 2. Thus, ϕ_{21} is called a mutual flux generated by the circuit 2. This case is the phenomenon how the magnetic coupling takes place between two individual circuits. This effect can be magnified or amplified by the increasing of wire number of coil. The power transfer efficiency of magnetic coupling can be increased by increasing the number of turns in the coil, the current magnitudes, the cross-sectional area of coil and the strength of radial magnetic field [43].

Based on above literature reviews, it was necessary to investigate the research on one of wireless power transfers (WPT), i.e. the magnetic inductive method, using photovoltaic solar cell source on various distances, coil turns and loads. This research was a new case regarding the photovoltaic solar panel and magnetic inductive wireless power transfer using an inverter on various loading conditions. The objectives of research were for designing of utilization of solar energy to be converted into electric energy, where the electric energy was transferred in wireless by the method of magnetic coupling. Furthermore, the voltage waveforms were investigated in order to obtain the relationship among the coil distance, turn number and load parameters. Besides that, the concerning on power and efficiency were also investigated in various conditions. The state of the art for this research was, especially, the analyses of wave forms, which were investigating the voltage waveform frequency spectra and magnitudes. The frequency spectra of waveforms were very important, as indications of the waveforms.

2. Research Method

In the beginning opinion, the existing wireless power transfers usually used resonance magnetic coupling due to efficiency reason. Nevertheless, it was too much harmonics, not applicable directly yet to the users and too many conversions so that, in authors' opinion, the efficiency became to be low. Therefore, it has been tried to investigate the wireless power transfer using inductive magnetic coupling, using the inverters and using 50 Hz power frequency. This was done with hope the efficiency would be higher tha previous ones, due to not to many conversions. However, in this research, the origin of voltage source was from **dc** voltage of photovoltaic or solar panel. Thus, it was also conversion existence from **dc** to **ac** voltages.

Figure 2 shows the classification of various wireless power transfer methods [44, 45]. Mainly, the wireless power transfer consists of two methods, namely electromagnetic induction and electromagnetic radiation. The former consists of electrodynamic induction and electrostatic induction. While, the latter consists of microwave/RF power and light/laser power. The electrodynamic induction consist of inductive coupling and magnetic resonant induction. Nevertheless, this research investigated in the inductive coupling category, as signed by the circle.

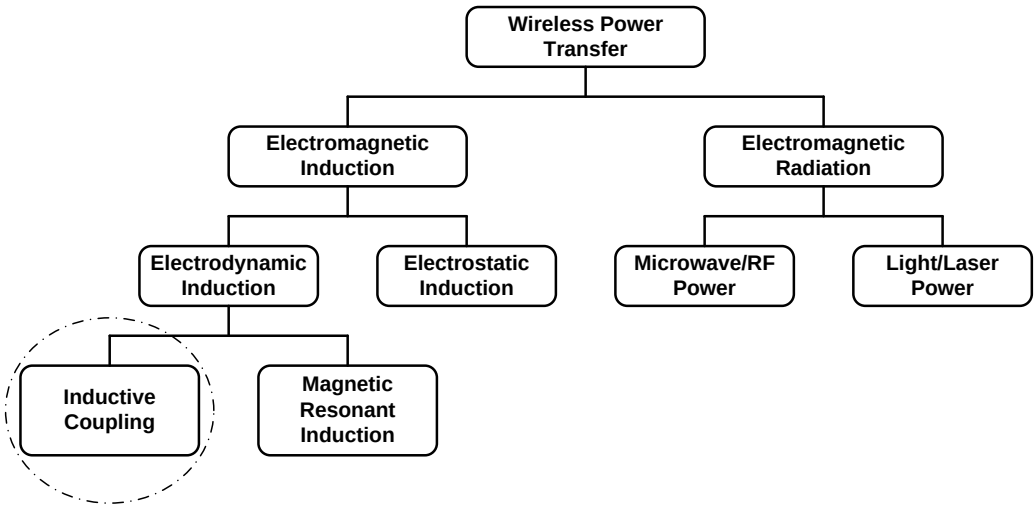

Fig. 2. The grouping of wireless power transfer.

Figure 3 shows the design of system on the wireless power transfer utilized the solar panel source on various load conditions. The figure illustrates the circuit plan for the experimental and measuring set-ups.

Initially, the generated electricity in the solar panel was converted into 50 Hz frequency of ac voltages. The solar panel changed the sun ray energy to electric energy, dc voltage and current, with the rating of 100 W_p of power. Furthermore, it was made some variations, such as the voltage, the distance between the sending and receiving coils, the loads and the number of coil turns. The variations of voltage were a variac (ac voltage variable), the variations of distance were used a ruler manually, the variations of load were used the various numbers of LED and the numbers of coil turns were used three pairs different coil numbers, namely 200, 400 and 600 turns. Thus, the research was conducted not only in one condition, but also in various conditions. As addition, the voltage waveforms were analyzed by using FFTs and THDs, and the magnitudes were analyzed by using nonlinear regression. The voltages on the transmitting and receiving coils were measured by the storage digital oscilloscope. The data of measurements were in **csv** files, which could be analyzed by Excel software and recorded in the form of **bmp** files.

From the photovoltaic panel, the electric currents would be flowed directly to the inverter or through the controller, and using a battery as back up. From the inverter, for regulating of voltage, it could be used by a regulating transformer or variac. Furthermore, the currents were flowed to the transmitter coil. Finally, the inductive voltages could be captured by the receiver coil, and the power supplied the LED lamps as the loads.

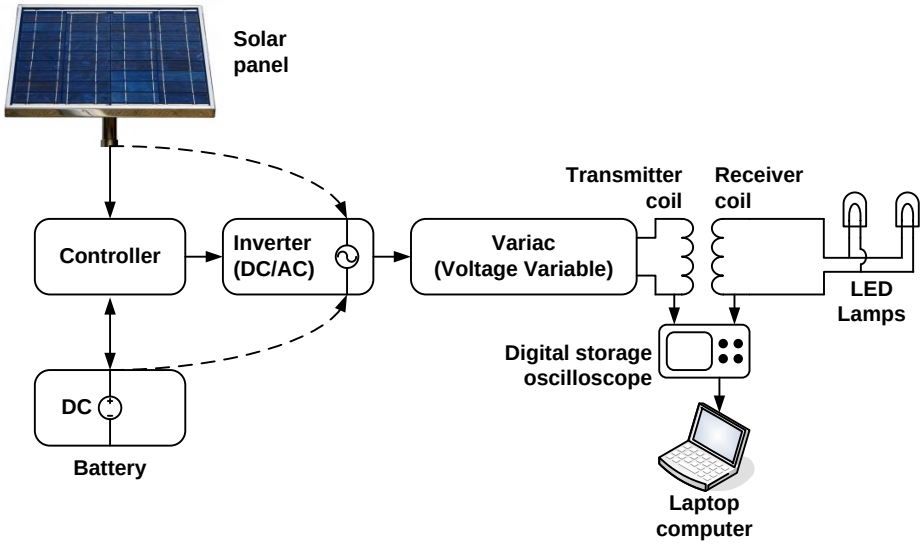

Fig. 3. The experimental and measuring set up.

The copper wires were for the composition of coils as the inductors. The inductors could store the electric energy. The pulleys were made of insulating material, used as the transmitter and receiver wrapped coils. The pulleys which picked the gaps and hollow, which could facilitate the wound copper wire and made it easy for electromagnetic field induction. Figure 4 shows the several pictures of implementation tools and equipment for the research experiments. These tools and equipment consisted of photovoltaic panel, transmitter and receiver coils, battery, controller and inverter, oscilloscope and a computer or laptop.

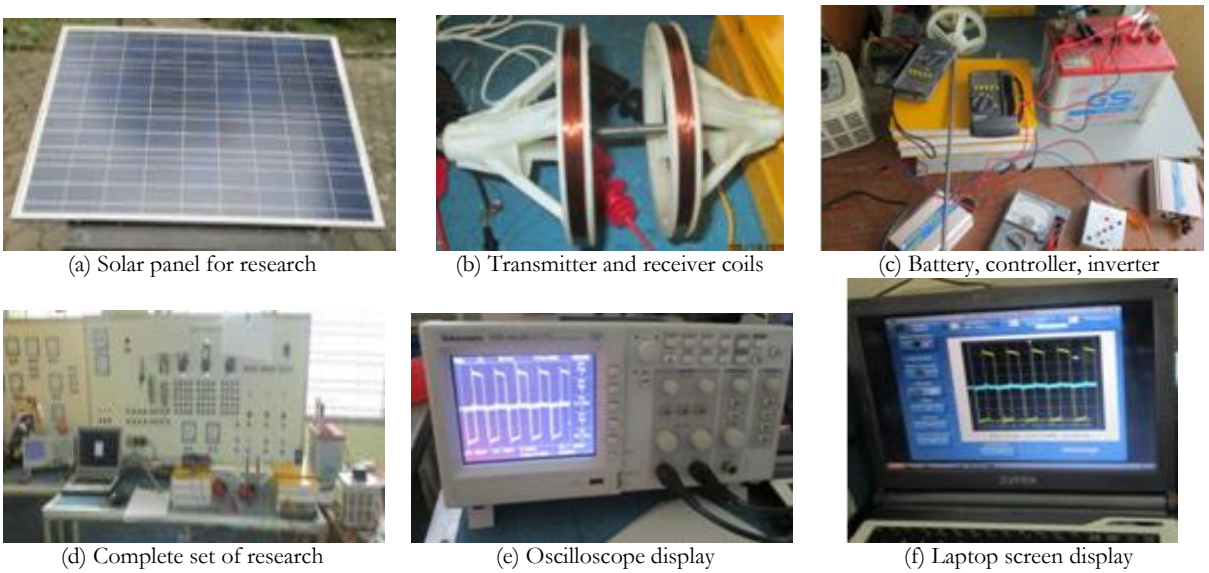

(a) Solar panel for research (b) Transmitter and receiver coils (c) Battery, controller, inverter

(d) Complete set of research (e) Oscilloscope display (f) Laptop screen display

Fig. 4. Several pictures of research experimental implementation.

For further analyses, the voltage waveforms were analyzed by using FFTs (fast fourier transforms) in order to obtain the frequency spectra. Therefore, it was necessary to calculate the THDs (total harmonics distortions) to obtain the characteristics of voltage waveforms [46].
The THD could be definition as [47]

$$THD = \frac{\sqrt{V_3^2+V_5^2+\cdots+V_{39}^2}}{V_1} \tag{3}$$

where V_1 is fundamental voltage magnitude and V_3 up to V_{39} are third up to thirty-nine were odd voltage harmonic magnitudes respectively which were calculated in this research. They were involved due to significant values. The data results for the receiver voltages due to the distance variations were approached by using the following equation, due to small deviations [48].

$$V_r = C\, e^{Ad} \tag{4}$$

where $\mathbf{V_r}$ was the receiver voltages (volts) and **d** was the distances between transmitter and receiver coils (cm). While, **A** and **C** were constants those should be found out, depend on the data. To obtain the equations, the data should be computed by using linearized least square method based on equation (4) with following equations.

$$A = \frac{n\sum V_{ri}\, d_i - \sum V_{ri}\sum d_i}{n\sum d_i^2 - (\sum d_i)(\sum d_i)^2} \tag{5}$$

$$B = \frac{1}{n}\left(\sum V_{ri} - A\sum d_i\right) \tag{6}$$

$$C = e^B \tag{7}$$

The sample Standard Deviation

$$s = \sqrt{\frac{1}{N}\sum_{i=1}^{N}(x_i - \bar{x})^2} \tag{8}$$

Finally, the trends of waveforms due to the variations could be discussed.

DOI:10.4186/ej.2018.22.4.121

3. Research Results and Discussion

The photovoltaic module characteristics that used in this research is listed in Table 1. it is shown that the maximum power was 100 watts and the voltage at maximum power was 17.5 volts. the standard test conditions (STC), the air mass coefficient of solar energy (AM) and the cell temperature were 1000 W/m2, 1.5 and 25°C respectively. this condition was almost universal when characterizing terrestrial power-generating panels [49].

Table 1. Photovoltaic module characteristics.

No.	Parameters	Quantities	Units
1	Maximum power (P_{max})	100	W
2	Voltage at maximum power (V_{mp})	17.5	V_{dc}
3	Open circuit voltage (V_{oc})	21.5	V_{dc}
4	Current at maximum power (I_{mp})	5.72	A
5	Short Circuit Current (I_{sc})	6.46	A
6	Maximum system voltage (V)	1000	V_{dc}
7	Maximum series fuse rating (A)	12	A
	At STC : 1000 W/m^2, AM : 1.5, Cell Temperature : 25°C		

Figure 5 shows scatter chart the duration of solar radiation in Bandung city, in 2017, that the data were obtained from The Geophysical Station of Bandung. The blanks meant there was not any data or measurable data. The average duration of solar radiation was **4.77** hours per day. Thus, it is proper enough to investigate a photovoltaic electric source to further application such as a wireless power transfer.

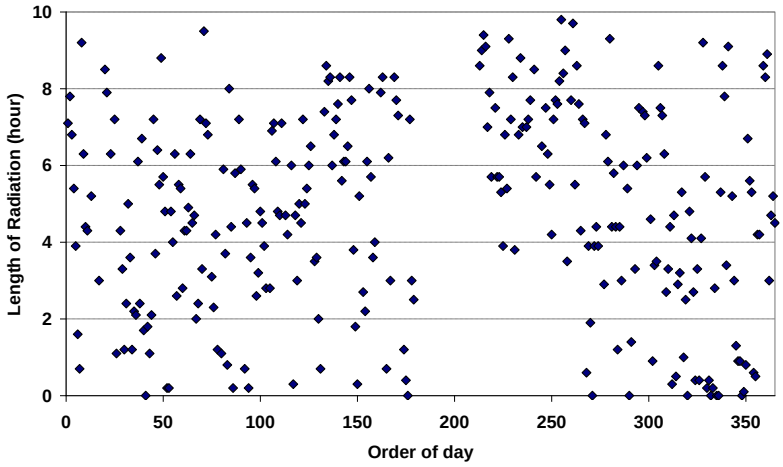

Fig. 5. Duration of solar radiation in 2017. (Source: The Geophysical Station of Bandung.)

On the other hand, from the test results of 100 W_p solar panel characteristics performed at Institut Teknologi Nasional Bandung, it was found that the maximum and minimum measured voltages on the photovoltaic module were 14.12 and 10.52 volts respectively. The maximum and minimum measured voltages on the battery were 13.56 and 10.48 volts respectively. The flowing current on the solar panel was always greater than the flowing current on the battery or the load. The maximum panel current ($I_{max\text{-}panel}$), the maximum battery current ($I_{max\text{-}battery}$) and the maximum load current ($I_{max\text{-}load}$) were 6.20 amperes, 4.43 A and 7.9 mA respectively. From the results above, it can be seen that the solar panel generated energy was always greater than the load used energy or the battery used charging. Nevertheless, of course, these values were obtained when the sun is always shining. However, if the sun was covered by the cloud, especially rain, the photovoltaic module could not supply the battery or the load properly. Based on the measurement sample in last condition, the solar panel, battery and load currents were 0.76 amperes, 0.129 amperes and 5.8 milliamperes resepectively.

Figure 6 shows the samples of photovoltaic panel characteristics, namely the panel voltages and currents on some days, i.e. 17th, 18th and 19th April 2018. In these days, the weathers were usually in rainy season. Therefore, the sunlight captured by the photovoltaic module was not optimal. The voltages would usually arise at around eight o'clock in the morning and decrease drastically at around four o'clock in the afternoon. The photovoltaic output voltages were only small variations, in range between 10.52 up to 14.12 volts. They would reach the high values in the range of about 11 until 13 o'clock. On the other hand, the trends of panel currents tended to follow the voltage patterns, such as increasing, decreasing, valleys and peak curves. The currents ranged between 0.76 up to 6.2 amperes.

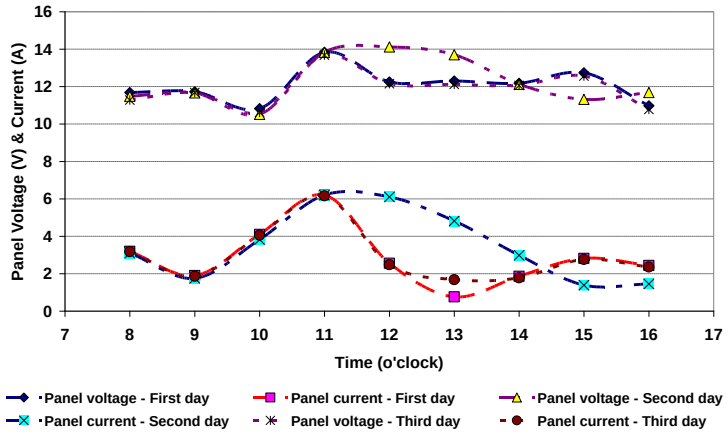

Fig. 6. Characteristic samples of photovoltaic module.

Figure 7 shows the waveforms for (a) 1 cm and (b) 15 cm of distances, on the 200 turns of transmitter and receiver coils. It could be observed that the amplitude of receiver voltage waveform for the distance of 1 cm was significantly higher than that 15 cm. This case was caused by the magnetic induction from transmitter to receiver coils was very high in that distance of 1 cm.

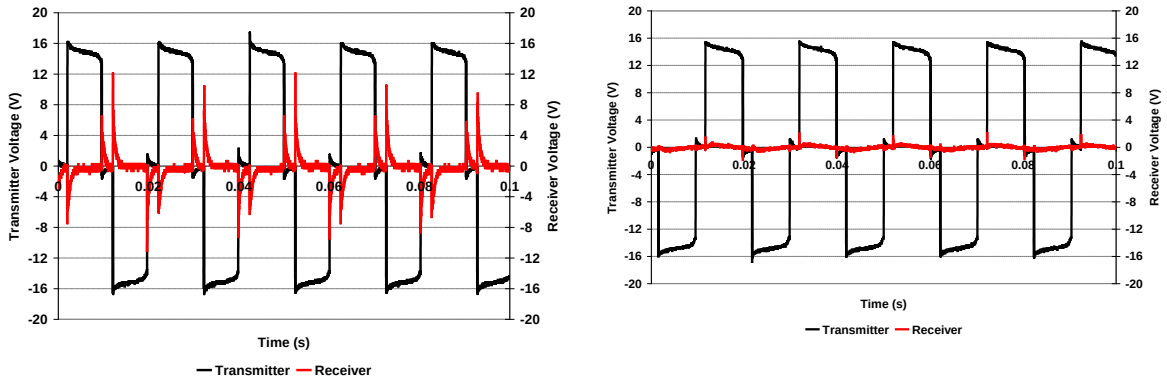

(a) 1 cm distance (b) 15 cm distance

Fig. 7. Typical waveforms for various distances on the 200 turns.

Figure 8(a) shows the frequency spectra of voltage waveforms for 1 cm, on the 200 turns of receiver coil. The transmitter voltage spectra were almost same due to the voltages were dominantly caused by the source, instead of caused by the receiver coils. After the fundamental, the significant harmonics magnitudes were order of 7th, 9th, 3rd, 17th, 15th and 5th respectively. Based on this condition, the THD would be very high. It could be calculated that the THD for receiver coil voltage was 110.58%.

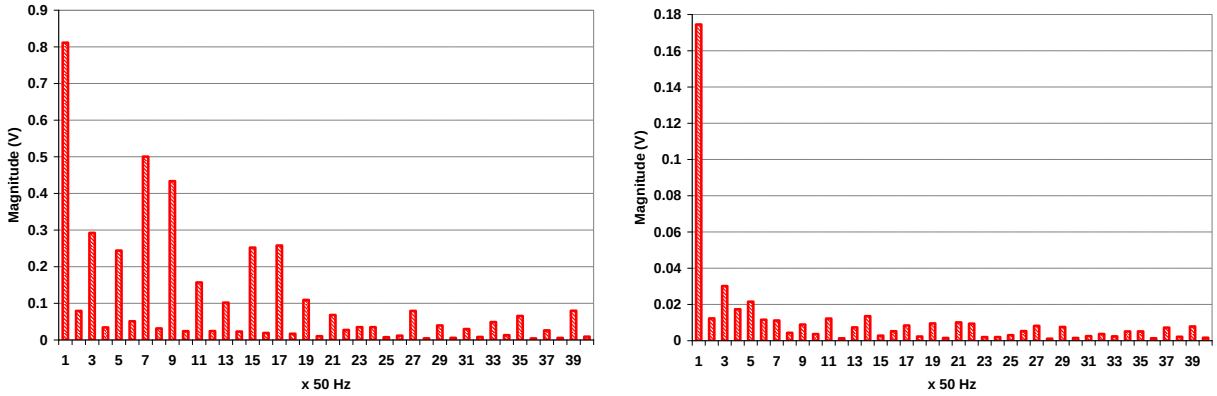

(a) 1 cm distance (b) 15 cm distance

Fig. 8. Frequency spectra for 1 cm and 15 cm distances on the 200 turns.

Figure 8(b) shows the frequency spectra of receiver voltage waveforms for 15 cm, on the 200 turns of transmitter and receiver coils. The harmonic magnitudes of receiver voltage were practically low. Therefore, the THD was also practically low. It could be calculated that the THD for receiver voltage was 33.20%.

Figure 9 shows the waveforms for (a) 1 cm and (b) 15 cm of distance, on 400 turns of transmitter and receiver coils. It could be observed that the amplitude of receiver voltage waveform for the distance of 1 cm was significantly high. This case was caused by the magnetic induction from the transmitter to the receiver coils was significantly high due to the location of coils was very close.

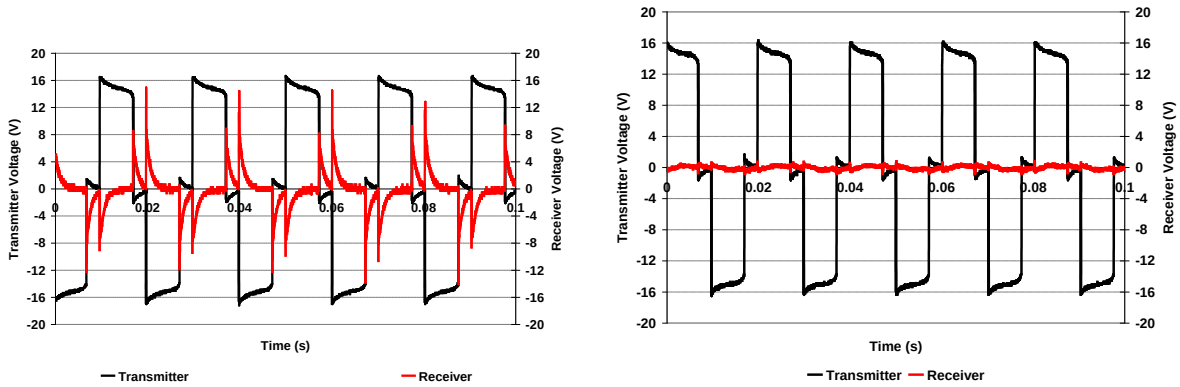

(a) 1 cm distance (b) 15 cm distance

Fig. 9. Typical waveforms for various distances on the 400 turns.

Figure 10(a) shows the frequency spectra of receiver voltage waveforms for 1 cm, on the 400 turns of receiver coil. In the receiver voltage, the significant harmonics were 7th, 5th, 9th, 15th and 13th orders. It could be calculated that the THD for receiver voltage was 76.42%.

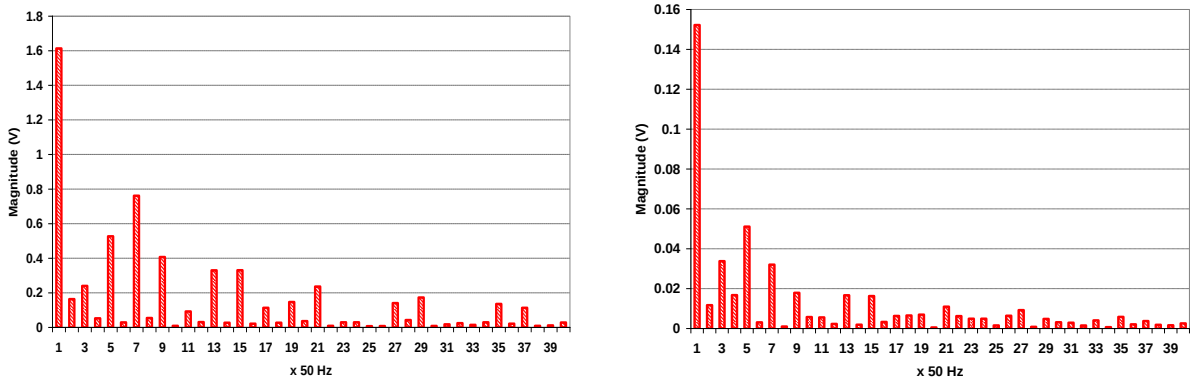

(a) 1 cm distance (b) 15 cm distance

Fig. 10. Frequency spectra for 1 cm and 15 cm distances on the 400 turns.

Figure 10(b) shows the frequency spectra of receiver voltage waveforms for 15 cm, on the 400 turns of receiver coil. The significant harmonics in the receiver voltage were 5th, 7th, 3rd, 9th, 13th and 15th orders. Thus, the total harmonics was high enough. It could be calculated that the THD for receiver voltage was 53.96%.

Figure 11 shows the voltage waveforms for (a) 1 cm and (b) 15 cm distance, on the 600 turns of transmitter or sender and receiver coils. It could be observed that the amplitude of waveform for the distance of 1 cm was significantly high. This case was caused by the magnetic induction from transmitter to receiver coils was significantly high due to the location of coils was very close.

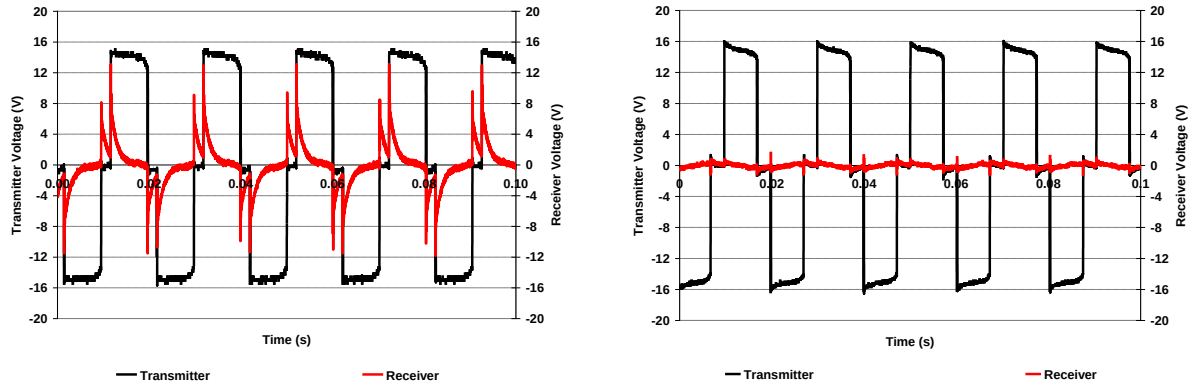

(a) 1 cm distance (b) 15 cm distance

Fig. 11. Typical waveforms for various distances on the 600 turns.

Figure 12(a) shows the frequency spectra of waveforms for 1 cm, on the 600 turns of receiver coil. The significant harmonics in the receiver voltage were 3rd, 9th, 11th and 7th orders. It could be calculated that the THD for receiver voltage was 60.03%.

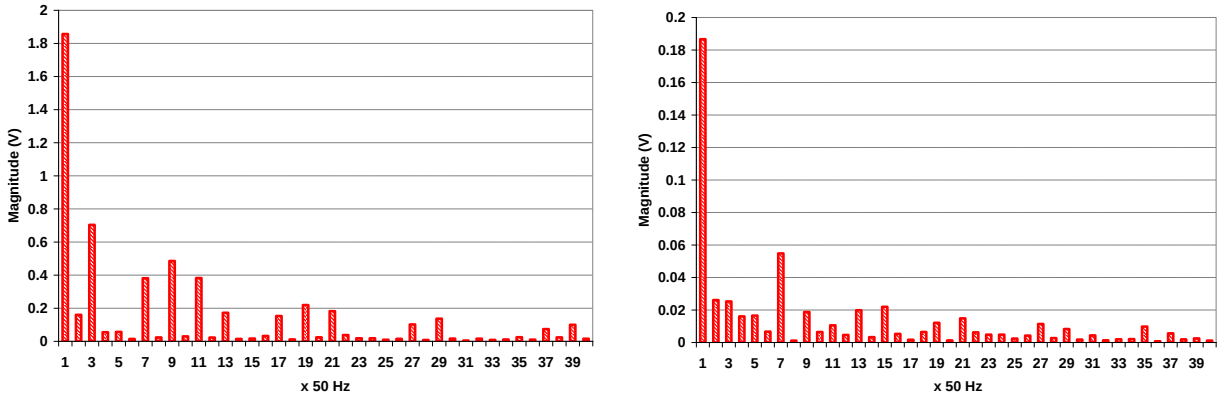

(a) 1 cm distance (b) 15 cm distance

Fig. 12. Frequency spectra for 1 cm and 15 cm distances on the 600 turns.

Figure 12(b) shows the frequency spectra of waveforms for 15 cm of distance, on the 600 turns of receiver coil. The considerable harmonics were 7th, 3rd, 13th and 15th orders. It could be calculated that the THD for receiver coil voltage was 45.61%.

Figure 13 shows the graphics for sender or transmitter and receiver voltage magnitudes and sender current versus distance on 600 turns. It could be observed that the receiver voltages would decrease significantly, hyperbolically, as the transmitter and receiver coil distances increased linearly. This case was caused by the magnetic induction from the transmitter to the receiver coils reduced drastically as the distances increased.

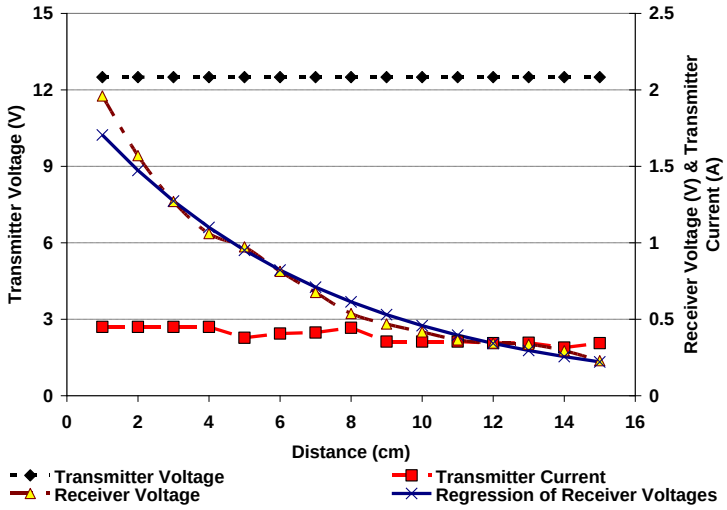

Fig. 13. Transmitter and receiver voltage magnitudes, and transmitter current versus distance on the 600 turns.

Figure 14 shows the transmitter and receiver powers as function of the distance on the 600-600 coil turns. The powers were the multiplication among the voltages, the electric currents and the power factors, where the latest referred to [50] as value of 0.99. As the distance increased, the transmitter power would drop gently. This case was caused by the reduction of back magnetic induction from the receiver coil that stay away from the transmitter coil. Thus, the current on the transmitter coil would reduce, and consequently, the power would also reduce. On the other hand, the receiver power would reduce drastically, more hyperbolically than the receiver voltage, as the distance increased. This case was caused by both the receiver voltage and current those also reduced drastically. As the consequence, the power curve would reduce more drastically than the voltage curve as the distance increased. Furthermore, the transferring efficiency on the receiver to the transmitter coil powers would reduce slightly as the distance between

transmitter and receiver coil increased. This efficiency was slight reduction, due to the beginning values were already low.

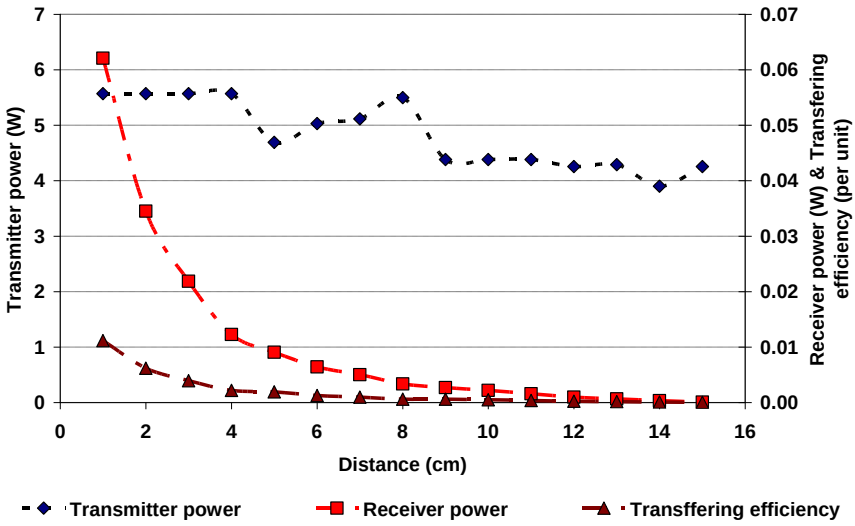

Fig. 14. Transmitter and receiver powers and transferring efficiency versus distance on the 600 turns.

Figure 15 shows the graphics for sender or transmitter and receiver voltage magnitudes and transmitter current versus distance on the 400 turns. It could be observed that the receiver voltages would decrease significantly, as the transmitter and receiver coil distances increased linearly. This phenomenon was caused by the magnetic induction between the transmitter and receiver coils reduced drastically as the distances increased linearly.

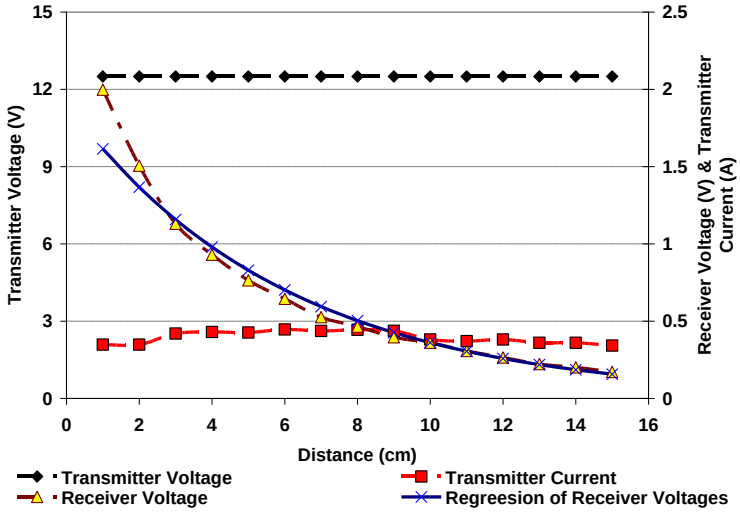

Fig. 15. Transmitter and receiver voltage magnitudes, and transmitter sender current versus distance on the 400 turns.

Figure 16 shows the transmitter and receiver power on the 400-400 coil turns as function of distance. The transmitter power would reduce more slightly rather than the previous one, the 600-600 coil turns. This case was caused by the back magnetic induction from the receiver coil that getting away from the transmitter coil and also lower magnetic induction due to lower coil turns compared to the previous one. However, the receiver power would also reduce drastically as the distance increased. Nevertheless, this reduction was very slightlier than the previous one, in Fig. 14. While, the transferring efficiency was almost

same as that the 600-600 coil turns, where it reduced slightly as the transmitter-receiver coil distance increased.

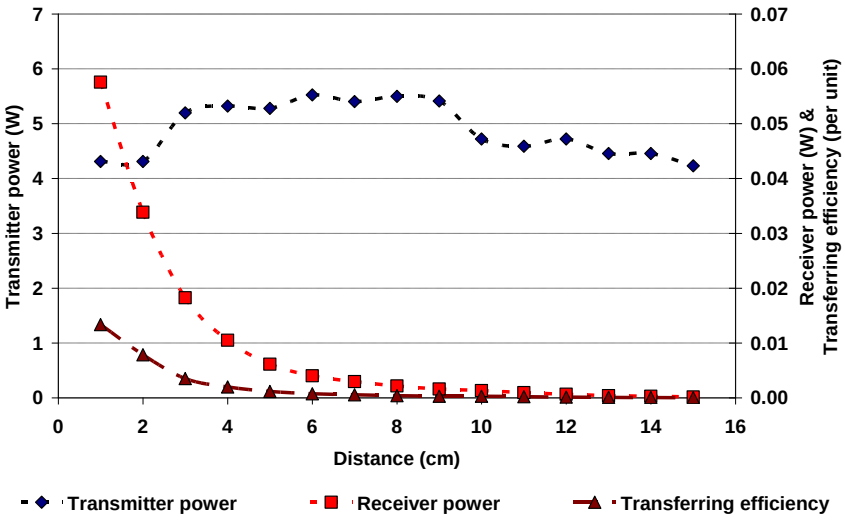

Fig. 16. Transmitter and receiver powers and transferring efficiency versus distance on the 400 turns.

Figure 17 shows the curves for transmitter and receiver voltage magnitudes and transmitter current versus distance on the 200 turns. It could be observed that the receiver voltage magnitudes would decrease considerably, as the transmitter and receiver coil distances increased linearly. Nevertheless, it was slighter than the previous ones, due to less of turn number.

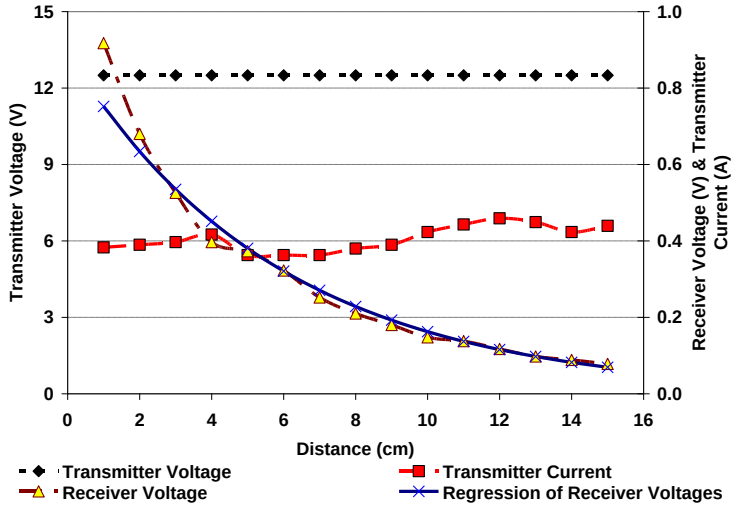

Fig. 17. Transmitter and receiver voltage magnitudes, and transmitter current versus distance on the 200 turns.

Figure 18 shows the transmitter and receiver power on the 200-200 coil turns as function of distance. The transmitter power would be constant, even tended to very slightly increase, as the distance increased. This case was probably caused by the low impedance of coil, due to the lowest turn number among the remaining coils. The low coil impedance made the low drop voltage in the coils. However, the receiver power would also reduce drastically as the distance increased. Nevertheless, this reduction was very slightlier than the previous ones, in Figs. 14 and 16. While, the transferring efficiency was around a half compared to that the 600-600 or 400-400 coil turns, and it reduced slightly as the transmitter-receiver coil distance increased.

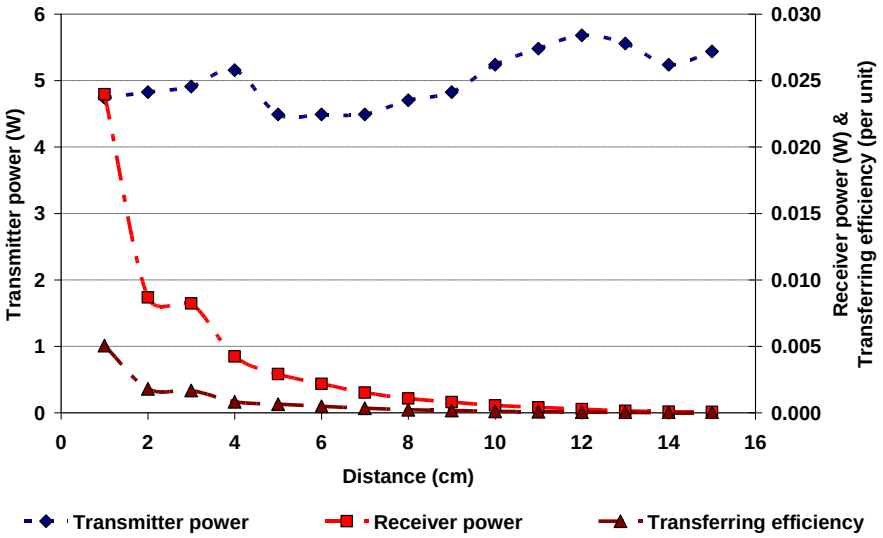

Fig. 18. Transmitter and receiver powers and transferring efficiency versus distance on the 200 turns.

The THDs of voltage waveforms for transmitter coils were fairly constant, with the average of 26.75. Otherwise, the THDs for receiver coils depended on the distances. If the transmitter and receiver coil distances were close, the THDs of voltage wave spectra tent to be high, and the vice versa, the THDs tent to be low. This case is listed in Table 1. Furthermore, as the distances increased, the receiver voltage THDs would reduce considerably. Thus, the receiver voltages would be close relatively to the pure sinusoidal waveform. As addition, the receiver voltage THDs would reduce as the coil turns increased. Therefore, the receiver voltage waveforms would be close to the pure sinusoidal waveform relatively as the coil turns increased. On other hand, the receiver voltage THDs would decrease significantly as the distances between the transmitter and receiver coils increased, with the decreasing average as 38.09% based on the three conditions of percent reductions. While, the THDs would reduce considerably as the turn decreased, as 25.28% for the 200 to 400 and 400 to 600 turns in the percent average on the distance of 1 cm.

Table 2 also indicates the regression functions these related between the voltage magnitudes and the distances for receiver coils. On the equations, generally, the magnitudes would rise as the coil turns increased. Besides that, on the high coil turns, the relating curves would be more declivous than those the low coil turns. This case was predicted that in the high coil turns, the generated electromotive forces would be high and vice versa. The data deviations compared to the regression results were still very low, those were under 15%.

Table 2. THDs for various distances.

Coil turns	Distance (cm)	Transmitter voltage THDs (%)	Receiver voltage THDs (%)	Regression function (V & cm)	Deviations (V)
200	1	25.55	110.58	$V_r = 0.891\, e^{-0.170d}$	**0.047**
	15	26.27	33.20		
400	1	30.57	76.42	$V_r = 1.907\, e^{-0.166d}$	**0.111**
	15	26.55	53.96		
600	1	25.20	60.03	$V_r = 1.973\, e^{-0.146d}$	**0.079**
	15	26.35	45.61		

It is shown that for the three turn numbers, the receiver voltage magnitudes would decrease drastically as the distances between the transmitter and receiver coils increased. The receiver voltage magnitudes would also decrease considerably as the turns reduced, with the average reductions as 0.095 volts and 0.357 volts, from 600 to 400 and 400 to 200 turn reductions respectively.

Figure 19 shows the waveforms for one and five lamps of load, on the 200 turns and 2 cm distance. It is shown that the transmitter voltage waveforms were similar, for both (a) one lamp of load and (b) five lamps of load. However, both receiver voltage waveforms and magnitudes were different, due to magnetic induction in the different distance.

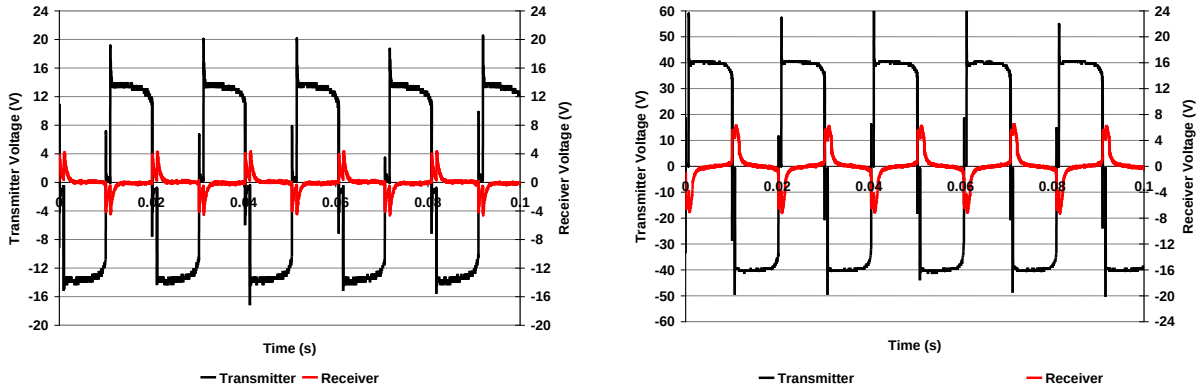

(a) one lamp (b) five lamps

Fig. 19. Typical waveforms for one and five lamps of load on the 200 turns and 2 cm distance.

Figure 20(a) shows the receiver voltage waveform frequency spectra for one lamp load on the 200 turns and 2 cm distance. The significant harmonics were 3rd, 5th, 19th,17th, 21st, 7th and 15th. It could be calculated that the THD for receiver voltage was 114.06%.

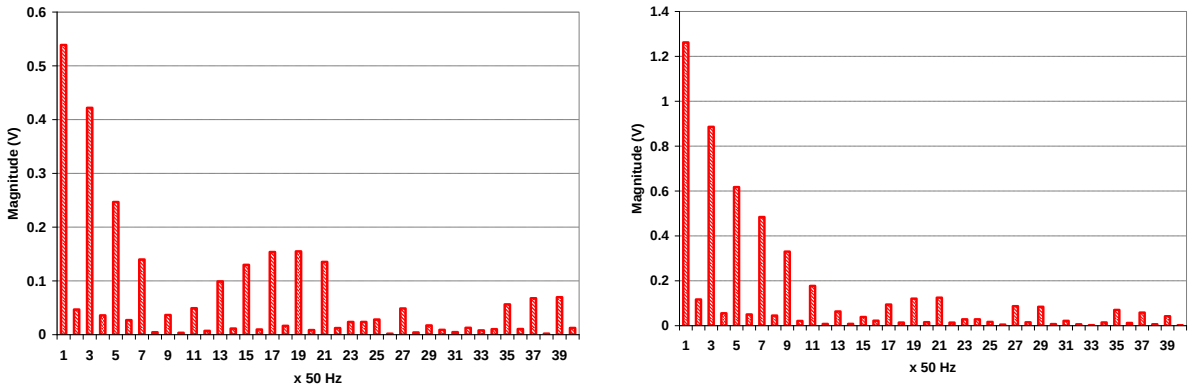

(a) One lamp load (b) Five lamp load

Fig. 20. Receiver voltage frequency spectra for one and five lamps of loads on the 200 turns and 2 cm distance.

Figure 20(b) shows the receiver voltage waveform frequency spectrum for five lamp load on the 200 turns and 2 cm distance. The significant harmonics were 3rd, 5th, 7th and 9th. It could be calculated that the THD for receiver voltage was 101.33%.

Figure 21 shows the waveforms for (a) one and (b) five lamp loads, on the 400 turns and 2 cm distance. The voltage magnitude of receiver coil was slightly reduced on the load of five lamps, rather than on the one lamp only. This phenomenon was caused by the occurrence of drop voltage, due to the loading current and impedance on the lines.

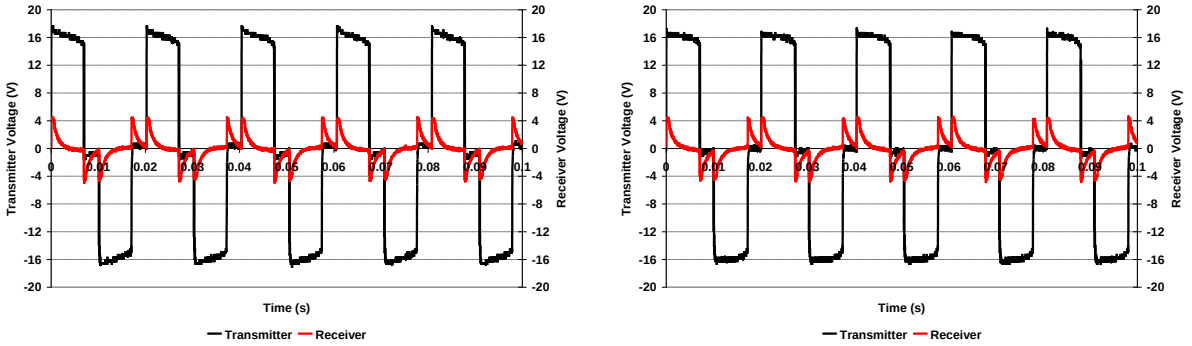

(a) One lamp (b) Five lamps

Fig. 21. Typical waveforms for various lamp loads on the 400 turns and 2 cm distance.

Figure 22(a) shows the frequency spectra of receiver voltage waveforms for one lamp load on the 400 turns and 2 cm. It could be calculated that the THD for receiver voltage was 73.96%.

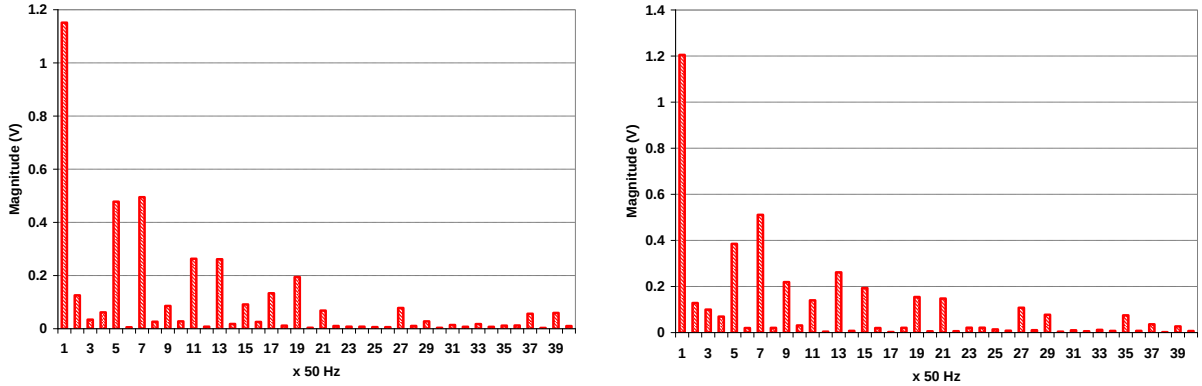

(a) one lamp load (b) five lamp load

Fig. 22. Frequency spectra of receiver voltage waveforms load on the 400 turns and 2 cm distance.

Figure 22(b) shows the frequency spectra of receiver voltage waveform for the five lamp load on the 400 turns and 2 cm distance. The significant harmonics were 7th, 5th, 13th, 5th and 19th orders. It could be calculated that the THD for receiver voltage waveform was 68.88%.

Figure 23 shows the transmitter and receiver voltage waveforms for one and five lamps, on the 600 turns and 2 cm distance. The receiver voltage magnitude on the five lamp load was lower than that on the one lamp load. This occurrence was caused by the drop voltages due to loading current and impedance on the lines.

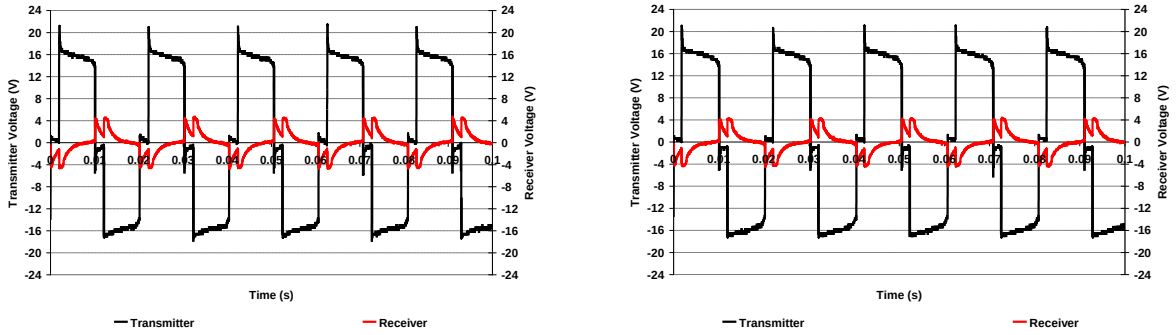

(a) one lamp (b) five lamps

Fig. 23. Typical waveforms for various lamp loads on the 600 turns and 2 cm distance.

Figure 24(a) shows the frequency spectra of receiver voltage waveform for the one lamp load on the 600 turns and 2 cm distance. The significant harmonics were 3rd, 9th, 7th and 11th. It could be calculated that the THD for receiver voltage was 55.41%.

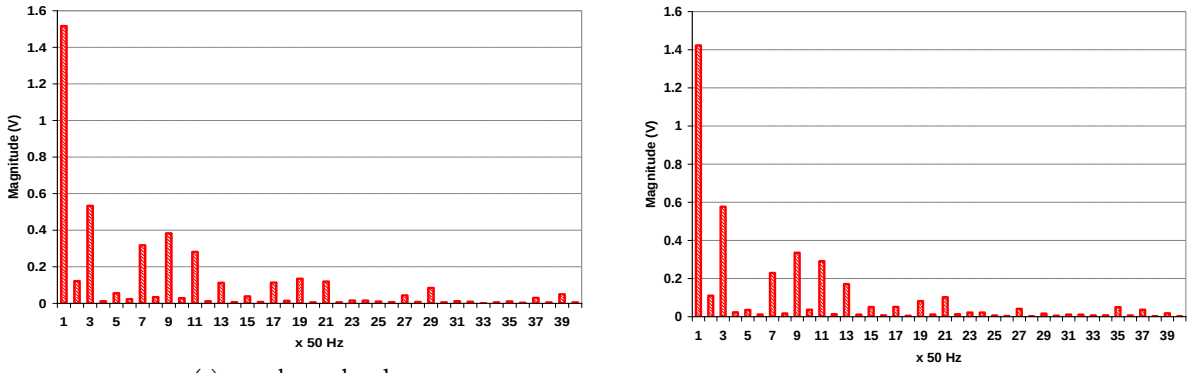

(a) one lamp load (b) five lamp load

Fig. 24. Frequency spectra of receiver voltage waveform on the 600 turns and 2 cm distance.

Figure 24(b) shows the frequency spectra of receiver voltage waveform for the five lamp load on the 600 turns and 2 cm distance. The considerable harmonics were 3rd, 9th, 11th, 7th and 13th orders. It could be calculated that the THD for receiver voltage was 57.00%.

Figure 25 shows the graphic for transmitter and receiver voltage amplitudes versus lamp number on the 200 turns. It was observed that the receiver voltage reduced slightly as the load of lamp number increased, and the transmitter voltage was maintained at the constant value. The average decline of receiver voltage amplitude due to the lamp loading was -23.34% as the constant transmitter voltage amplitudes of 13.2 Volt.

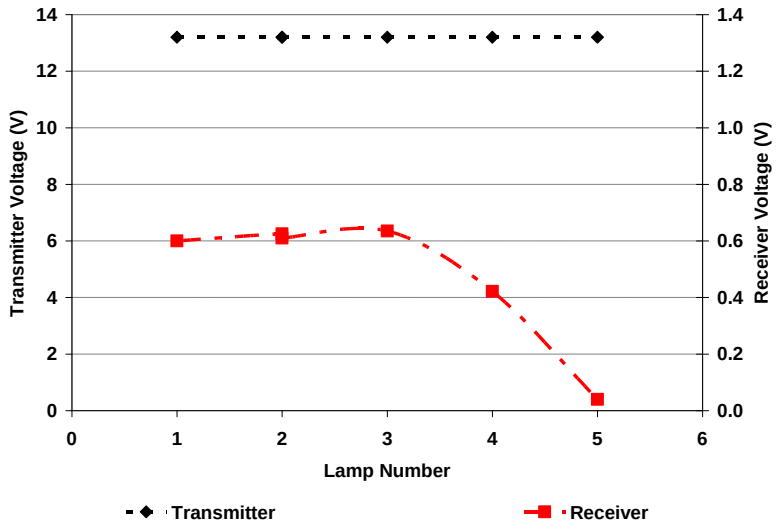

Fig. 25. Transmitter and receiver voltages versus lamp number on the 200 turns of coil.

Figure 26 shows the graphics for the transmitter and receiver voltage amplitudes versus lamp number on the 400 turns of coil. As it was observed that the receiver voltage reduced slightly as the load of lamp number increased, and where the transmitter voltage was maintained at the constant value. The average decline of receiver voltage amplitude due to the lamp loading was -0.56% as the constant transmitter voltage amplitudes of 12.5 Volt.

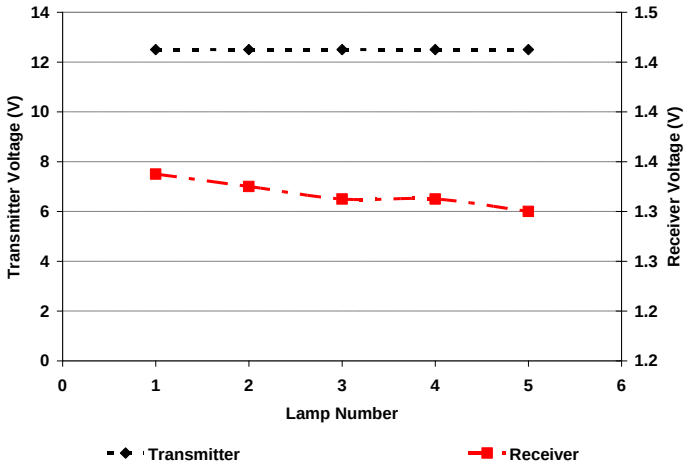

Fig. 26. Transmitter and receiver voltage amplitudes versus lamp number on the 400 turns.

Figure 27 shows the graphics for the transmitter and receiver voltage amplitudes versus lamp number on the 600 turns. As it was observed that the receiver voltage reduced slightly as the load of lamp number increased, and if the sender voltage was maintained a constant value. The average decline of receiver voltage amplitude due to the lamp loading was -1.96% as the constant transmitter voltage amplitudes of 13.5 Volt.

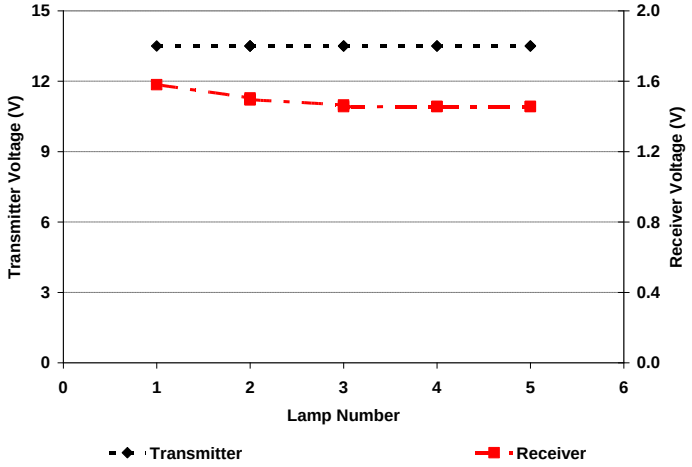

Fig. 27. Transmitter and receiver voltage amplitudes versus lamp number on the 600 turns.

Base on the three coils of loadings, the declines of the receiver voltage amplitudes would be smaller on the high coil turns. This case indicated that the higher coil turns, the receiver coil voltage would be more immune to the loadings.

Table 3 lists the THDs on various LED lamps as the loads. As the load increased, the THDs would decrease slightly. From one to five lamps, the THDs reduced up to 12.73%. While, the THDs reduced due to coil turn numbers were between 11.88% up to 40.1%, for 200, 400 and 600 coil turns. Thus, the receiver voltage harmonics were dominantly influenced by the coil numbers, rather than the loads. The receiver voltage THDs reduced significantly as the coil numbers increased. The voltage magnitudes would decrease slightly as the load increased where from one to five lamps, the voltage reductions were 0.489, 1.334 and 1.482 volts respectively for 200, 400 and 600 turns.

Table 3. THDs for various loads.

Coil turns	Lamps (pcs)	Transmitter voltage THDs (%)	Receiver voltage THDs (%)
200	1	30.67	114.06
	5	34.50	101.33
400	1	26.28	73.96
	5	25.06	68.88
600	1	26.86	55.41
	5	26.44	57.00

Figure 28 shows the voltage waveforms for (a) 1.4 Volt rms and (b) 5.2 Volt, for voltage variation. It is roughly shown that the receiver voltage would, on the lower one, to be far from the pure sinusoidal waveform. Otherwise, the high amplitude, the waveforms were close to be sinusoidal waveform relatively.

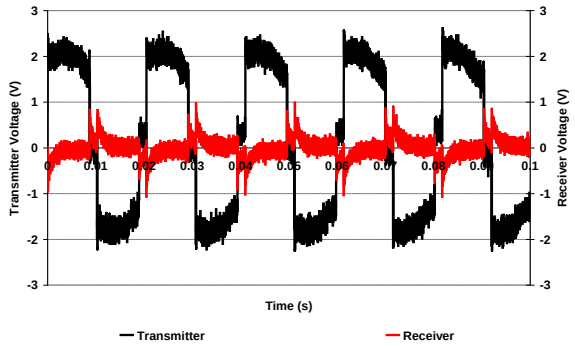

(a) 1.4 Volt rms of transmitter voltage

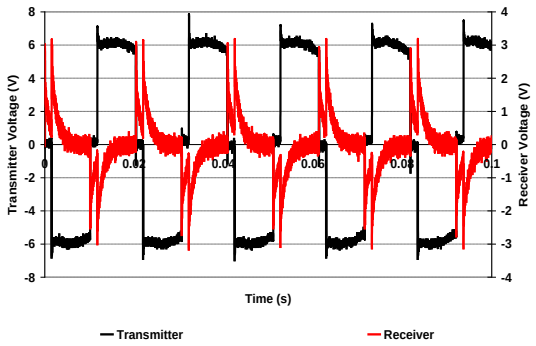

(b) 5.2 Volt rms of transmitter voltage

Fig. 28. Typical waveforms for various voltage magnitudes.

Figure 29(a) shows the frequency spectrum of receiver voltage waveforms for 1.4 Volt rms and 5.2 Volt rms of sender voltages. The considerable harmonics were 3rd, 9th, 11th, 7th and 13th orders. It could be calculated that the THD for receiver voltage was 64.45%.

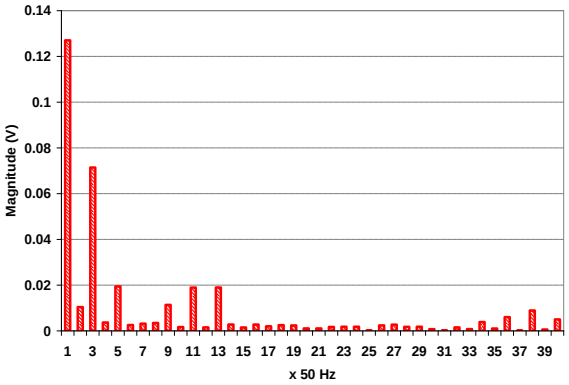

(a) 1.4 volts rms of transmitter voltage

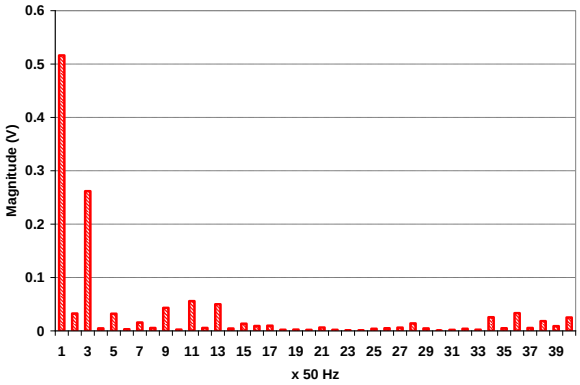

(b) 5.2 volts rms of transmitter voltage

Fig. 29. Frequency spectra of receiver voltage waveforms.

Figure 29(b) shows the frequency spectra of waveforms for 5.2 volt of transmitter voltage. The considerable harmonics were 3rd, 11th, 13th, and 9th orders. The calculated THD for receiver voltage was 55.47%.

Table 4 lists the THDs of transmitter and receiver voltage waveforms on the two samples of voltage amplitudes. The receiver voltage THDs would reduce as the voltage amplitudes increased. For this case,

from 1.4 to 5.4 V volts rms of the transmitter voltages, the THDs reduced up to 13.93%. It was very considerable. Therefore, the high of voltage amplitudes, the voltage waveforms would tend to be pure sinusoidal.

Table 4. THDs for various voltages.

Voltage (V)	Transmitter voltage THDs(%)	Receiver voltage THDs(%)
1.4	23.35	64.45
5.2	24.34	55.47

Figure 30 shows the graphic plot for receiver versus harmonics voltage magnitudes. It could be observed that the receiver voltage magnitudes increased steep linearly as the transmitter voltage magnitudes increased. Nevertheless, the receiver voltages were considerably lower than the transmitter ones, by the average ratio on the receiver to transmitter voltage magnitudes as **9.30**. On other hand, the THDs of receiver voltages would reduce considerably as the transmitter voltage magnitudes increased, with 8.98% reduction for 1.4 to 5.2 volts of the transmitter voltage magnitudes.

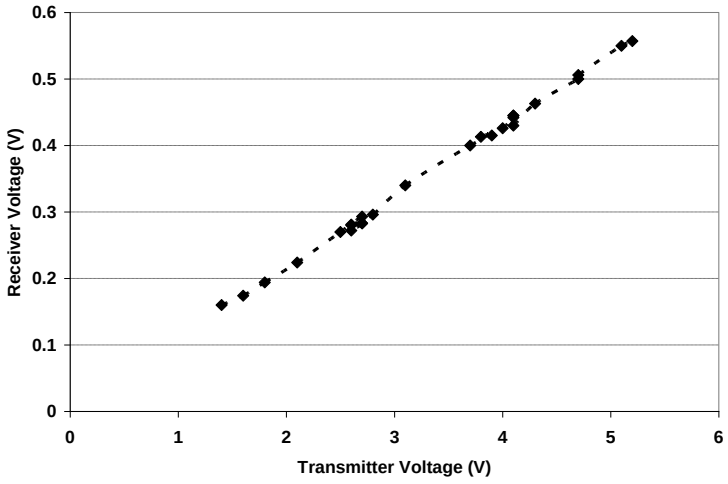

Fig. 30. Receiver versus transmitter voltage magnitudes.

Figure 31 shows the efficiency against to LED numbers of burden. These data were obtained on the photovoltaic panel voltage ranged 12.5 up to 14.1 volts, so that it could be said relatively constant. Efficiency would rise as the LED numbers increased, as increasing burden, and so that the current would increase too. Nevertheless, the increasing efficiency would be saturated as constant values.

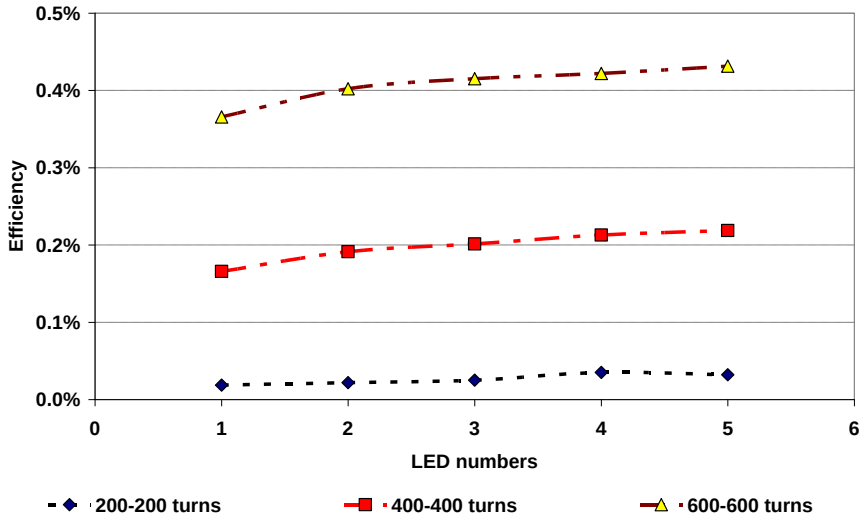

Fig. 31. Efficiencies versus LED numbers on various turn number.

Figure 32 shows the transmitter and receiver power versus the LED numbers as function the burden. Both transmitter and receiver powers would very slightly increase as the additional LED numbers of burden. This phenomenon was probably caused by the addition of LED would only made the small increasing current, due to the rating power of LEDs was very small, that was only 0.1 watt.

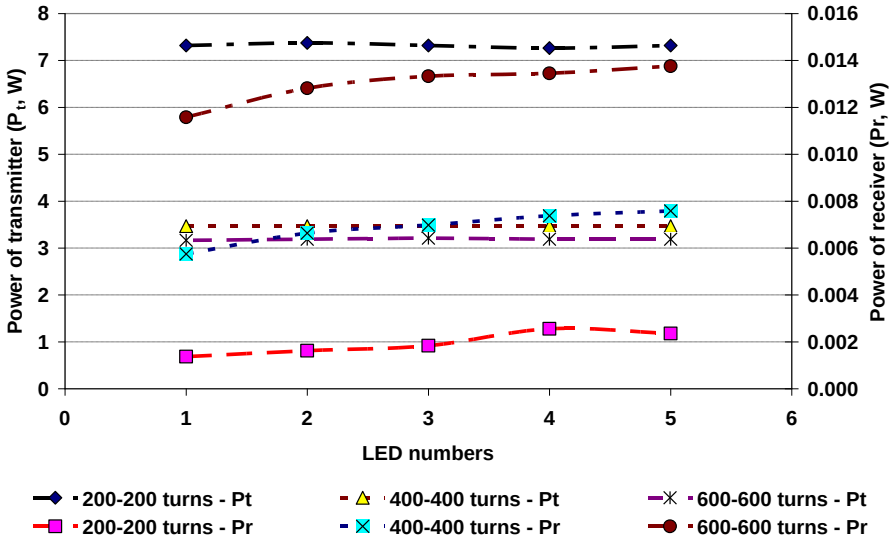

Fig. 32. Powers versus LED numbers on various turn number.

Figure 33 shows the efficiency curves as function of the turn number on five LED burden numbers. Generally, the efficiency would rise significantly as the coil turns increased. Otherwise, the efficiency would also rise as the LED number increased. Nevertheless, the latter was significantly lighter than that the former.

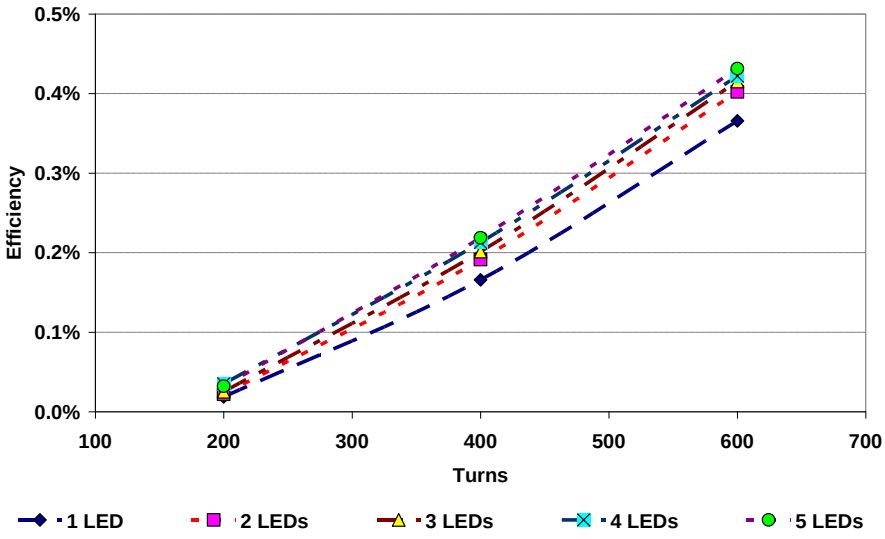

Fig. 33. Efficiency versus turn numbers on various LED burden numbers.

Figure 34 shows the curves on the transmitter power, receiver voltage and efficiency versus the transmitter voltage.

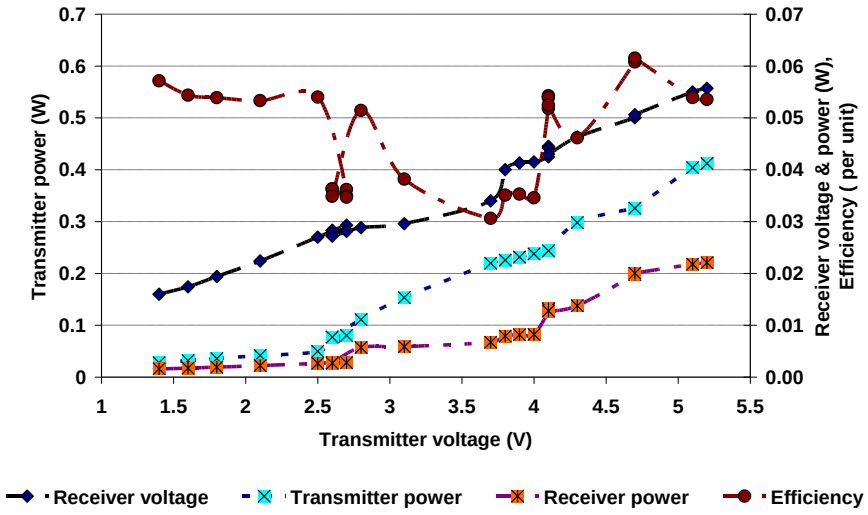

Fig. 34. Powers, receiver voltage and efficiency versus transmitter voltage on 600-600 turns.

Refer to previous one [45] and based these research results, the voltage, current and power on the receiver coils were depended drastically on the transmitter and receiver coil distances, significantly on the number of coil turns and slightly on the burdens. The first two parameters were dominantly caused by the magnetic field induction in the coils, and the last parameter was dominantly caused by the voltage drops, due to electric currents and impedances. The parameters those to be concerned in wireless power transfer system are system performance, time, cost, losses, reliability and safety. The system performance was moderate, where it was necessary the voltage system to be fairly constant or to be in certain range. The time taken to switch on the system was less due to not always in switch on condition. In the small scale or laboratory scale, the cost was high. As an example, based on the conducted research, it was required around USD 250, excluding the photovoltaic module. The losses were very high, where it was indicated by very low efficiency. The reliability was same as the system performance as moderate. Nevertheless, it was higher in safety. For the example, it was short circuit occurred in the transmitter system side, the photovoltaic module was most likely still safe, also depended on the magnitude of short circuit current. Besides that, in

this case, the magnetic inductions were still in safe condition. This was different from if changed directly to the alternating current voltage which cause a probably electrocution. The conditions on above parameters were in wireless power transfer, compared to the wired system. Of course, in this wired system, the conditions were in vice versa.

4. Conclusion

From the experiments using the solar panel source and inverter, with the frequency of 50 Hz, it could be obtained that the transfer power in wireless could operate properly. The receiver voltage magnitudes would decrease drastically, in hyperbolic curves, as the distances between the transmitter and receiver coils increased. The receiver voltage magnitudes would decrease considerably as the turns reduced, with the average reductions as 0.095 and 0.357 volts, from 600 to 400 and 400 to 200 turn reductions respectively. The THDs in the transmitter voltages were fairly constant, as average of 26.75%. Nevertheless, the receiver voltage THDs would decrease significantly as the distances increased, with decreasing average as 38.09% of the three condition percentage reductions. While, the THDs would reduce considerably as the turns decreased, as 25.28% of percent average for the 200 to 400 and 400 to 600 turns on the one cm of distance. Otherwise, the voltage magnitudes would decrease as the loads increased where from one to five lamp loads, as 0.489, 1.334 and 1.482 volts reductions for 200, 400 and 600 turns respectively. The THDs would decrease slightly as the loads increased, with the reducing average of 5.4% from one to five lamp loads, for the three conditions of turns. The receiver voltage magnitudes would increase steep linearly, with the average ratio of one per 9.30 as the transmitter voltage magnitudes increased. Nevertheless, the THDs of receiver voltages would reduce considerably as the transmitter voltage magnitudes increased, with 8.98% reduction for 1.4 to 5.2 volts of the transmitter voltage magnitudes.

The receiver power would reduce more drastically, compared to the above voltages, as the distance increased. This case was caused which the powers were influenced by both electric voltage and current. The efficiency would also reduce drastically as the distance increased. Nevertheless, it was gentler than the power, because the early values have already been low. Both parameters were significantly influenced by the coil turns, which the efficiency would be lower as the coil turns reduced. Based on the research results, the maximum transferring efficiency was **0.0615.** The efficiency would slightly increase, and tended to be saturated toward a certain value as the load increased. Therefore, most likely, in the future, the coil turns should be increased.

Acknowledments

We would like to express the deepest appreciation to The Geophysical Station of Bandung for providing the data and The Institute for Research and Community Service, Institut Teknologi Nasional Bandung (Itenas), which has supported the funding in the research.

Nomenclatures

A,B,C,D : constants that need to be obtained
AC : alternating current
bmp : bitmap image
csv : comma-separated values
d : variable of distance
DC : direct current

e : Euler's number (2.718…)
emf : electromotive force
FFT : Fast Fourier transform
i_1 : electric current in circuit 1
i_2 : electric current in circuit 2
i (subsribe) : order of data
kWh : kilo Watt hour
LED : light-emitting diode

P_t : power of transmitter
P_r : power of receiver
s : standard deviation
THD : total harmonic distortion
V_1 : fundamental voltage magnitude
V_3, V_5, . . . , V_{39} : odd order from third to thirty-nine voltage harmonics
Variac : AC voltage variable
V_r : voltage based on regression
W_p : watt peak
ϕ_1 : linkage magnetic flux in coil 1
ϕ_{11} : linkage magnetic flux in coil 1 against coil 1
ϕ_{12} : linkage magnetic flux in coil 2 against coil 1
ϕ_2 : linkage magnetic flux in coil 2
ϕ_{21} : linkage magnetic flux in coil 1 against coil 2

m^2 : square meter
MW : mega watt
n : number of data
ϕ_{22} : linkage magnetic flux in coil 2 against coil 2
θ_1 : phase angle on circuit 1
θ_2 : phase angle on circuit 2

References

[1] N. S. Kumara, "Solar home power scale and urban availability in Indonesia," (in Indonesian), *Teknologi Elektro*, vol. 9, no. 1, pp. 68-75, Jan.-Jun. 2010.

[2] J. Custer and J. Lianda, "Analysis of solar energy utilization as source of energy in housing category R1 900 VA in Bengkalis Island," (in Indonesian) in *Proceedings of the National Seminar on Industry and Technology*, 26 Dec. 2012, pp. 17-22.

[3] I. Rahardjo and I. Fitriana, "Analysis of the potential of solar power in Indonesia, national electricity supply strategy in order to anticipate the utilization of small scale coal power plant," (in Indonesian), *Nuclear Power Plant and Renewable Energy*, pp.43-51, 2015.

[4] A. Lubis, "Renewable energy in sustainable development," (in Indonesian) *Journal of Environmental Engineering*, vol. 8, no. 2, pp. 156-163, May 2007.

[5] Marwani, "Potential use of solar energy stoves for household needs," (in Indonesian) in *Proceedings of National Seminar AvoER ke-3*, Palembang, 26-27 Oct. 2011, pp. 85-94.

[6] KRT, "Reaching '*Indonesia Bisa*', Hybrid Electric Energy Technology in Bantul," (in Indonesian) DIY, Ministry of Research and Technology, 2010.

[7] T. K. Nugraha, "Solar panels solutions for the region are rich in solar energy resources, but must feel the dark night due to power supply," (in Indonesian) presented at *The 3rd Indonesia EBTKE-ConEx*, Jakarta, June 4-6th, 2014.

[8] D. M. Rahman, N. B. Sakhawat, R. Amin, and F. Ahmed, "A study on renewable energy as a sustainable alternative for ensuring energy security in Bangladesh and related socio-economic aspects," *Engineering Journal*, vol. 16, no. 2, pp. 47-52, Apr. 2012.

[9] M. Arulkumaran and W. Christraj, "Experimental analysis of non tracking solar parabolic dish concentrating system for steam generation," *Engineering Journal*, vol. 16, no. 2, pp. 53-60, Apr. 2012.

[10] S. B. Adejuyigbe, B. O. Bolaji, M. U. Olanipekun, and M. R. Adu, "Development of a solar photovoltaic power system to generate electricity for office appliances," *Engineering Journal*, vol. 17, no. 1, pp. 29-39, Jan. 2013.

[11] P. Sirinamaratana and E. Leelarasmee, "Diagnosis through series connected photovoltaic panels by pulse power line communication technique," *Engineering Journal*, vol. 19, no. 5, pp. 13-27, Oct. 2015.

[12] S. R. Thakare, A. N. Shire, and U. S. Jawarkar, "Study and overview of wireless transmission of electrical power," *International Journal of Research in Science and Engineering (IJRISE)*, vol. 1, no. 3, pp. 15-20, May 2015.

[13] A. Gopinath, "All about transferring power wirelessly," *Power Transfer, Electronics for You*, pp. 52-56, Aug. 2013.

[14] R. Dhara, "Wireless power transmission," *International Journal of Multidisciplinary Research and Development*, vol. 2, no. 8, pp. 458-461, Aug. 2015.

[15] S. S. Valtchev, E.N. Baikova, and L. R. Jorge, "Electromagnetic field as the wireless transporter of energy," *Facta Universitatis, Ser. Elec. Energ.*, vol. 25, no. 3, pp. 171-181, Dec. 2012.

[16] S. K. Singh, T. S. Hasarmani, and R. M. Holmukhe, "Wireless transmission of electrical power overview of recent research and development," *International Journal of Computer and Electrical Engineering*, vol. 4, no. 2, pp. 207-211, Apr. 2012.

[17] V. Singh, P. Singh, and S. Kumar, "Introduction to wireless power transmission," *International Journal of Technology Innovations and Research*, vol. 8, pp. 1-10, Mar. 2014.

[18] B. R. Randy, M. Hariharan, and R. A. Kumar, "Secured wireless power transmission using radio frequency signal," *International Journal of Information Sciences and Techniques (IJIST)*, vol. 4, no. 3, pp. 115-122, May 2014.

[19] A. Mahmood, A. Ismail, Z. Zaman, H. Fakhar, Z. Najam, M. S. Hasan, and S. H. Ahmed, "A comparative study of wireless power transmission techniques," *Journal of Basic and Applied Scientific Research*, vol. 4, no. 1, pp. 321-326, 2014.

[20] A. Mahmood, H. Fakhar, S. H. Ahmed, and N. Javaid, "Analysis of wireless power transmission," presented at *The International Industrial and Information Systems Conference (IIISC)*, Chiang Mai, Thailand, 2014.
[21] Y. N. Burali and C. B. Patil, "Wireless electricity transmission based on electromagnetic and resonance magnetic coupling," *International Journal of Computational Engineering Research*, vol. 2, no. 7, pp. 48-51, Nov. 2012.
[22] S. Abdelhady, "An entropy approach to Tesla's discovery of wireless power transmission," *Journal of Electromagnetic Analysis and Application*, vol. 5, pp. 157-161, 2013.
[23] G. N. Reddy and G. J. U. Reddy, "Effect of wireless electricity on human bodies," *International Journal of Engineering Trends and Technology, (IJETT)*, vol. 4, no. 6, pp. 2567-2569, Jun. 2013.
[24] T. Sawant, D. Pilankar, R. Sule, and S. Mahadeshwar, "An overview of technological advancements and future possibilities in wireless power transmission," *International Journal of Research in Engineering and Technology (IJRET)*, vol. 2, no. 8, pp. 260-267, Aug. 2013.
[25] S. Aldhaher, C.-K. Luk, and F. Whidborne, "Tuning class E inverters applied in inductive links using saturable reactors," *IEEE Transaction on Power Electronics*, vol. 29, no. 6, pp. 2969-2978, Jun. 2014.
[26] S. Aldhaher, P. C. K. Luk, K. E. K. Drissi, and J. F. Whidborne, "High input voltage high frequency class E rectifiers for resonant inductive links," *IEEE Transaction on Power Electronics*, no. 99, pp. 1-9, 2014.
[27] S. Aldhaher, P. C. K. Luk, A. Bati, and J. F. Whidborne, "Wireless power transfer using class e inverter with saturable DC-feed inductor," *IEEE Transactions on Industry Application*, vol. 50, no. 4, pp. 2710-2718, Jul./Aug. 2014.
[28] S. Aldhaher, P. C. K. Luk, and J. F. Whidborne, "Electronic tuning of misaligned coils in wireless power transfer systems," *IEEE Transactions on Power Electronics*, vol. 29, no. 11, pp. 5975-5982, Nov. 2014.
[29] D. Chaurasia and S. Ahirwar, "A review on wireless electricity transmission techniques, current trends in technology and science," vol. 2, no. 4, pp. 298-300, 2013.
[30] K. Harakawa, "Wireless power transmission at rotating and sliding elements by using the capacitive coupling technology," presented at *2014 Automotive Simulation World Congress*, Monday October 06, 2014.
[31] A. V. Kumar, P. Niklesh, and T. Naveen, "Wireless power transmission," *International Journal of Engineering Research and Application (IJERA)*, vol. 1, no. 4, pp. 1306-1310, Nov.-Dec. 2011.
[32] K. Kalyan, S. A. Mohsin, and A. Suresh, "Transmission of power through wireless systems," *International Journal of Engineering and Advanced Technology (IJEAT)*, vol. 2, no. 4, pp. 394-398, Apr. 2013.
[33] M. F. Razik, H. T. O. Silem, A. M. Akl. Omnia, Y. M. A. Alradi, M. E. Elbtity, Y. Atef, A. A. Mohammed, and Z. Elmasry. *Applying Wireless Power Transfer on Charging Portable Devices* [Online]. Available: www.researchgate.net/publication [Accessed: April 11, 2015]
[34] S. Pawade, T. Nimje, and D. Diwase, "Goodbye wires: Approach to wireless power transmission," *International Journal of Emerging Technology and Advanced Engineering*, vol. 2, no. 4, pp. 382-387, Apr. 2012.
[35] R. Biswa, "Feasibility of wireless power transmission," Seminar Report, Electronics and Communication Engineering, College of Science and Technology, Rinchending, Phuentsholing, pp. 1-23, May 2012.
[36] T. K. Mandal, "Wireless transmission of electricity—Development and possibility," in *Proc. Sixth International Symposium Nikola Tesla*, Belgrade, SASA, Serbia, October 18-20, 2006, pp. 1-4.
[37] M. Shidujaman, H. Samani, and M. Arif, "Wireless power transmission trends, 2014," in *IEEE International Conference on Informatics, Electronics and Vision (ICIEV)*, 23-24 May 2014, Dhaka, pp. 1-6.
[38] N. K. Garg and R. S. Meena, "Wireless transmission network: A imagine," *International Journal of Scientific, Engineering and Technology*, vol. 2, no. 5, pp. 362-365, May 2013.
[39] S. A. Khidri, A. A. Malik, and S. H. Memon, "WiTricity: A wireless energy solution available at anytime and anywhere," *International Journal of Engineering Research and General Science*, vol. 2, no. 5, pp. 26-34, Aug.-Sept. 2014.
[40] O. Oyepeju, C. Mkasanga, and J. Das. *A Feasibility Study of Wireless Charging* [Online] Available: www.academia.edu [Accessed: Sept. 2015]
[41] M. F. Salbani, M. A. A. Halim, A. H. Jahidin, and M. S. A. M. Ali, "Helical antenna design for wireless power transmission: A preliminary study," in *IEEE International Conference on System Engineering and Technology (ICSET)*, 2011, pp. 192-195.

[42] H. M. Dighade and A. A. Nimje, "Wireless power transmission using satellite based solar power system," *International Journal of Application or Innovation in Engineering and Management (IJAIEM)*, vol. 2, no. 10, pp. 86-91, Oct. 2013.
[43] S. D. Gupta, M. S. Islam, K. M. Nuronnabi, M. S. Hossain, and M. Z. Hasan, "Design and implementation of cost effective wireless power transmission model: Good bye wires," *International Journal of Scientific and Research Publication*, vol. 2, no. 12, pp. 1-9, Dec. 2012.
[44] K. Siddabattula. *Why Not A Wire? The Case for Wireless Power, TESLA Wireless Power Solutions* [Online]. Texas Instruments. Available: https://www.wirelesspowerconsortium.com [Accessed: April 11th, 2018]
[45] V. Thakur and S. Abrol, "Wireless power transfer application and its comparison with wire short distance transmission," *International Refereed Journal of Scientific Research in Engineering (IRJSRE)*, vol. 2, no. 2, pp. 1-6, Feb. 2017.
[46] OriginLab Coporation. (2002). *Topography of an Origin Project and Workspace, Chapter 2: Origin Basics* [Online]. Available: http://hacol13.physik.uni-freiburg.de/fp/Literatur/Origin [Accessed on April 11th, 2018.
[47] T. M. Blooming and D. J. Carnovale, "Application of IEEE STD 519-1992 harmonic limits," in *Pulp and Paper Industry Technical Conference 2006, Conference Record of Annual*, Appleton, WI, USA, 18-23 June 2006, pp. 1-9.
[48] J. H. Mathews and K. D. Fink, *Numerical Methods Using Matlab*, 3rd ed. Prentice Hall, 1999, pp. 252-309.
[49] Wikipedia. (2018). *Air Mass (Solar Energy)* [Online]. Available: https://en.wikipedia.org/wiki/Air_mass_(solar_energy) [Accessed: April 14th, 2018]
[50] C. A. Cheng, C. H. Chang, H. L. Cheng, C. H. Tseng, and T. Y. Chung, "A single-stage high-power-factor light-emitting diode (LED) driver with coupled inductors for streetlight applications," *Applied Sciences*, vol. 7, no. 167, pp. 1-18, 2017.